Commun. Comput. Chem.
doi: 10.4208/cicc.2013.v1.n4.6

Vol.**1**, No.**4**, pp. 351-361
December 2013

REGULAR ARTICLE

Extensive Ab initio Study on the Low-lying Excited States of SiBr$^+$ Including Spin-Orbit Coupling

Hong-Sheng Zhai, Xiao-Mei Zhang and Yu-Fang Liu*

College of Physics and Electronic Engineering, Henan Normal University, Xinxiang 453007, China

Received 23 Sep 2013; Accepted (in revised version) 26 Nov 2013

Abstract: The entire 12 Λ-S electronic states of SiBr+ cation are calculated with high-level ab initio caculation in which electronic structure internally contracted multi-reference configuration interaction plus Davidson correction (MRCI+Q) method at the level of aug-cc-pVTZ, where Douglas-Kroll scalar relativistic effect is taken into account as well. The spin-orbit coupling (SOC) effect is introduced to make these 12 Λ-S electronic states split into 23 Ω states. The potential energy curves (PECs) of Λ-S and Ω states are depicted with the aid of the avoid crossing rule between the same symmetry. The shapes of Ω states are different from these of the original Λ-S states because of the avoiding crossing rules of the same symmetry. Based on the obtained PECs, the spectroscopic constants of Λ-S states and Ω states are determined, most of the PECs for Ω states are no longer smooth and the corresponding spectroscopic constants are not easy determined. The transition dipole moments (TDMs) of the transitions from several excited Ω states of 0^+ and 1 symmetries to the ground state X0^+ are predicted as well.

AMS subject classifications: 81Q05, 35Q40, 58Z05

Key words: MRCI(+Q), Spin–orbit coupling (SOC) effect, Potential energy curve (PEC), Spectroscopic constant, Predissociation

Introduction

The silicon-containing molecules and ions are particularly important due to their importance in many fields of physics and chemistry, especially applications in the plasma and surface physics [1, 2]. As one of them, silicon monobromide cation could be found in large number

---

* Corresponding author. *Email address*: yf-liu@henannu.edu.cn (Y.-F. Liu)

in the reactive $SiBr_4$ environment [3, 4] and the accurate electronic structure of the $SiBr^+$ could therefore be conducive to explore the reactive mechanism in the $SiBr_4$ environment. However, to the best of our knowledge, the accurate data for the electron structure of $SiBr^+$ still in shortage. So far, only few early experimental studies on $SiBr^+$ have been reported [3-5].

The early experiment date of spectra for $SiBr^+$ summarized by Huber and Herzberg [5] barely centers on the spectroscopic constants (T_e, ω_e and $\omega_e\chi_e$) of one low-lying excited state with ground state, and the corresponding irreducible representations and spin multiplicities of these two electronic states were not given. The emissions $a^3\Pi_{0+}$-$X^1\Sigma^+$ and $a^3\Pi_1$-$X^1\Sigma^+$ of $SiBr^+$ were detected and identified by Tsuji *et al.* [4] in He, Ne, and Ar afterglows in the region from 335 to 380nm. In their work, the partial spectroscopic constants for electronic state $a^3\Pi_1$ and $X^1\Sigma^+$ were obtained. Later, Ishiguro *et al.* [5] launched the study of microwave spectra on $SiBr^+$, where the microwave spectrum of $SiBr^+$ with its isotopic species were observed in a free-space cell by a discharge through pure $SiBr_4$ gas. At last, only the spectroscopic constants R_e and B_e of ground state for $SiBr^+$ were determined. It is also well known that the spin-orbit coupling SOC effect plays an important role in the spectroscopy and dynamics of molecules. Especially at the dissociation limit of $SiBr^+$, experimental data show that the ground ^2P_u state of the Br atom is split by 3685cm^{-1}. This strongly affects the shape of the potential energy curves PECs and dissociation energy of $SiBr^+$. Moreover, electronic wavefunctions for the electronic states of the diatomic molecule are often dominated by more than one electronic configuration of multiconfigurational wavefunctions.

Here, the spin-orbit coupling effect (SOC) is introduced into the calculations by drawing support from the full Breit-Pauli Hamiltonian operator (H_{BP}) after the MRCI+Q calculation. The state interaction is employed in our SOC calculations, which means that the SOC eigenstates are obtained by diagonalizing the matrixes $H_{el}+H_{so}$ in the basis of eigenfunction of H_{el}. In the process, the H_{el} and H_{so} are obtained from MRCI+Q calculations and CASSCF wave functions, respectively. The SOC potential energy curves are drawn with the aid of the avoided crossing rule of the same symmetry. Based on the potential energy curves of the bound Λ-S and Ω states, the spectroscopic constants, including the equilibrium inter-nuclear distance (R_e), the excited energy (T_e), the vibrational constants (ω_e and $\omega_e\chi_e$), the balance rotation constant (B_e). The dissociation energies (D_e) are obtained by comparing the molecular energy at the equilibrium inter-nuclear distance and at a large separation. Based on the above, the multi-reference configuration interaction (MRCI) method is selected to perform the current work. In this paper, the entire 12 Λ-S states of $SiBr^+$ are calculated and the scalar relativistic effects are also considered in the calculation. The spin-orbit coupling effect is taken into account to make the original calculated 12 Λ-S states split and recombine to 23 Ω states. Based on the calculated potential energy curves (PECs) of Λ-S states and Ω states, the spectroscopic constants are determined by the LEVEL 8.0 program [7], which is in good agreement with the experimental values. The transition dipole moments from the excited Ω states to ground state are predicted. The Frank-Condon factors and radiative lifetimes of the transitions are evaluated as well.

Computational details

The whole ***ab initio*** calculations on the electronic structure of $SiBr^+$ cation are performed through the quantum chemistry MOLPRO 2008.1 program package [6]. The spectroscopic constants are determined with the aid of the LEVEL 8.0 program [7].

The single-point energy calculations are carried out to obtain the potential energy curves (PECs) of Λ-S electronic states, where the Gaussian-type all-electron augmented correlation consistent polarized valence quadruple zeta basis sets [aug-cc-pVTZ] are selected for atoms Si[16s10p3d2f] and Br[21s14p10d2f] in the calculations of Λ-S states.

In order to obtain the high-level PECs of $SiBr^+$, the potential energies of a series of bond lengths are calculated according to three steps as follows: first, the restricted Hartree-Fock (RHF) method is selected to produce the ground-state single-configuration wavefunction. Then, the multi-configuration wavefunction is calculated with the state-averaged complete active space self-consistent field (SA-CASSCF) method [8, 9]. Finally, the internally contracted multi-reference configuration interaction (MRCI) approach [10, 11] is employed to launch the correlation energy calculation and achieve the accurate energies based on the acquired optimized reference wavefunction in the SA-CASSCF calculation. At the same time, the calculation is extended to including the relativistic effect and Davidson modification(+Q) to improve the level of the PECs, where the one-electron integral second-order Douglas-Kroll integrals is used to evaluate the Scalar relativistic effect and Davidson modification is employed to correct the size-extensivity of truncated CI. The potential energy curves (PECs) of these 12 Λ-S electronic states are drawn with aid of the avoided crossing rule of the same symmetry.

Because of self-limit of the MOLPRO program, C_{2v} point group symmetry, the subgroup of the $C_{\infty v}$ point group, is adopted in the calculation of electronic structure, which holds A1/B1/B2/A2 irreducible representations. For $SiBr^+$, 5a1, 2b1 and 2b2 symmetry molecular orbitals (MOs) are determined as the active space, which correspond to the atoms Si 3s3p4s and Br 4s4p shells in the SA-CASSCF and subsequent MRCI+Q calculation. The outermost $3s^2 3p^1$ electrons of Si^+ and $4s^2 4p^5$ electrons of Br are placed in the active space, and 10 electrons of 3d shell are placed in the closed shell in which the electron orbitals are doubly occupied in all reference configuration state functions but are correlated through single and double excitations. Namely, there are totally 20 electrons of $SiBr^+$ radical used in the calculation of electronic correlation energy.

The spin-orbit coupling (SOC) effect is introduced in the present work by drawing support from the full Breit-Pauli Hamiltonian operator (H_{BP}) after the MRCI calculation, where the state interaction method is employed [12]. Through the above calculation, calculated 12 Λ-S electronic states split and recombine to 23 Ω electronic states. The SOC potential energy curves are plotted with the aid of the avoided crossing rule of the same symmetry.

Table 1 The spectroscopic constants of Λ-S state

Λ-S State		T_e/cm^{-1}	R_e/Å	ω_e/cm^{-1}	$\omega_e\chi_e$/cm^{-1}	B_e/cm^{-1}	D_e/eV	*Main Electron Configuration/%*
$X^1\Sigma^+$		0	2.1206	523.7323	1.5447	0.1809	4.5996	$1\sigma^2 2\sigma^2 3\sigma^2 4\sigma^0 5\sigma^0 1\pi^4 2\pi^0$(80.0) $1\sigma^2 2\sigma^2 3\sigma^2 4\sigma^0 5\sigma^0 1\pi^{\alpha\beta\alpha} 2\pi^\beta$(5.1) $1\sigma^2 2\sigma^2 3\sigma^\alpha 4\sigma^\beta 5\sigma^0 1\pi^4 2\pi^0$(1.4)
	Exp^a	0		533.3±1.8	1.5±0.7			
	Exp^b	0		535.8	1.6			
$^3\Sigma^+$(I)		28371.46	2.5875	236.3596	1.5156	0.1215	1.1003	$1\sigma^2 2\sigma^2 3\sigma^2 4\sigma^0 5\sigma^0 1\pi^{\alpha\beta\alpha} 2\pi^\alpha$(87.0)
$a^3\Pi$		28878.92	2.1750	418.3058	5.5510	0.1719	1.0205	$1\sigma^2 2\sigma^2 3\sigma^\alpha 4\sigma^0 5\sigma^0 1\pi^4 2\pi^\alpha$(83.5) $1\sigma^2 2\sigma^2 3\sigma^\alpha 4\sigma^0 5\sigma^0 1\pi^{\alpha\beta\beta} 2\pi^{\alpha\alpha}$(1.5) $1\sigma^2 2\sigma^2 3\sigma^0 4\sigma^\alpha 5\sigma^0 1\pi^4 2\pi^\alpha$(1.4)
	Exp^b	29005.4		428.7	6.9			
$^3\Delta$		29456.79	2.6430	220.3096	1.5208	0.1164	0.9652	$1\sigma^2 2\sigma^2 3\sigma^2 4\sigma^0 5\sigma^0 1\pi^{\alpha\beta\alpha} 2\pi^\alpha$(87.5)
$A^1\Pi$		36051.09	3.9215	54.7046	0.8738	0.0529	0.08835	$1\sigma^2 2\sigma^2 3\sigma^2 4\sigma^\alpha 5\sigma^0 1\pi^{\alpha\beta\beta} 2\pi^0$ (86.5)
	Well(II)	**36387.03**	**2.7730**	**83.3824**	**1.8775**	**0.1060**	**0.0467**	$\mathbf{1\sigma^2 2\sigma^2 3\sigma^\alpha 4\sigma^0 5\sigma^0 1\pi^4 2\pi^\beta}$**(85.3)**
$^1\Delta$		29825.46	2.6925	212.2630	1.4782	0.1122	0.9186	$1\sigma^2 2\sigma^2 3\sigma^2 4\sigma^0 5\sigma^0 1\pi^{\alpha\beta\alpha} 2\pi^\beta$(86.9)
$^1\Sigma^-$		29948.72	2.6880	211.1791	1.4848	0.1126	0.9006	$1\sigma^2 2\sigma^2 3\sigma^2 4\sigma^0 5\sigma^0 1\pi^{\alpha\beta\alpha} 2\pi^\beta$(87.3)
$^3\Sigma^-$		30168.42	2.6895	209.4737	1.5298	0.1125	0.8772	$1\sigma^2 2\sigma^2 3\sigma^2 4\sigma^0 5\sigma^0 1\pi^{\alpha\beta\alpha} 2\pi^\alpha$(87.3)
$^1\Sigma^+$(II)		33651.65	2.9265	158.9142	1.3686	0.0950	0.4167	$1\sigma^2 2\sigma^2 3\sigma^2 4\sigma^0 5\sigma^0 1\pi^{\alpha\beta\alpha} 2\pi^\beta$(60.9) $1\sigma^2 2\sigma^2 3\sigma^\alpha 4\sigma^\beta 5\sigma^0 1\pi^4 2\pi^0$(19.1) $1\sigma^2 2\sigma^2 3\sigma^2 4\sigma^0 5\sigma^0 1\pi^4 2\pi^0$(7.0)
$^3\Pi$(II)		36434.76	3.3225	143.1207	6.8327	0.0738	0.0921	$1\sigma^2 2\sigma^2 3\sigma^2 4\sigma^\alpha 5\sigma^0 1\pi^{\alpha\beta\alpha} 2\pi^0$(50.8) $1\sigma^2 2\sigma^2 3\sigma^\alpha 4\sigma^0 5\sigma^0 1\pi^4 2\pi^\alpha$(37.1)
$^1\Pi$(II)		36561.97	3.4190	101.2414	8.2042	0.0697	0.03299	$1\sigma^2 2\sigma^2 3\sigma^\alpha 4\sigma^0 5\sigma^0 1\pi^4 2\pi^\beta$(57.9) $1\sigma^2 2\sigma^2 3\sigma^2 4\sigma^\alpha 5\sigma^0 1\pi^{\alpha\beta\beta} 2\pi^0$ (29.9)

^{a}Ref[3] ^{b}Ref[5]

Based on the PECs of the Λ-S and Ω electronic states, the spectroscopic constants, including equilibrium internuclear distance R_e, excitation energy T_e, vibrational constants ω_e and $\omega_e\chi_e$, balanced rotation constant B_e, are determined by numerical solution of the one-dimensional nuclear Schrödinger equation. The dissociation energy D_e was obtained by subtracting the molecular energy at R_e from the energy at a large separation. The Frank-Condon factors of the transitions from the low-lying bound Ω electronic states to the ground Ω state are also calculated by using the LEVEL program 8.0.

Results and discussion

a. The PECs and spectroscopic constants of Λ-S states

The full 12 Λ-S states correlated to the dissociation limit of ground atom state $Si^+(^2P_u)+Br(^2P_u)$ are calculated at the theoretical level of MRCI+Q/AVTZ plus scalar relativistic effect. According to the avoided crossing rule of the same symmetry, the corresponding potential energy curves of these 12 Λ-S states are plotted in **Fig. 1** , in which only the $^3\Sigma^+$(II) state is fully repulsive. The spectroscopic constants of the bound states are determined and presented in **Table 1**, where the main electron configurations at the equilibrium position are given as well.

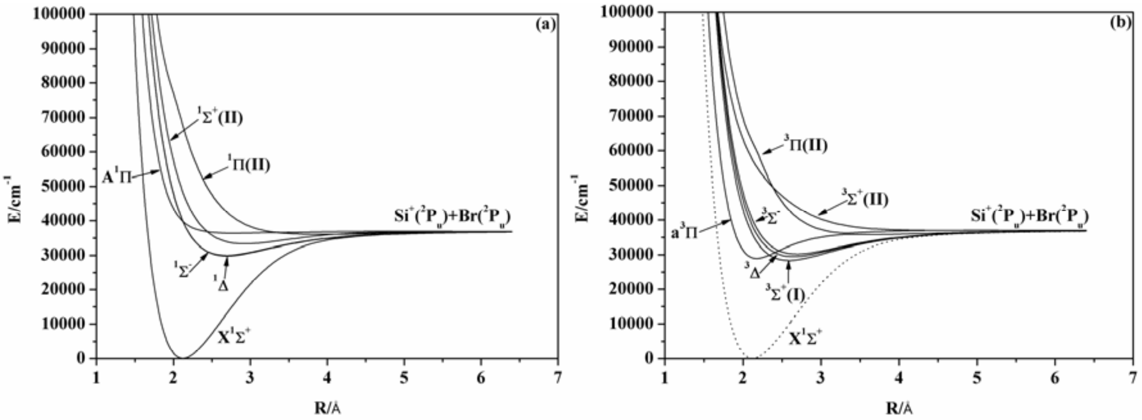

Fig. 1: The PECs for the 12 Λ-S states of $SiBr^+$ cation as functions of internuclear distance R: (a) the singlet states (b) the triplet states.

The ground state $X^1\Sigma^+$ of $SiBr^+$ radical mainly characterizes the electronic configuration $1\sigma^2 2\sigma^2 3\sigma^2 4\sigma^0 5\sigma^0 1\pi^4 2\pi^0$ and holds the potential well with a depth of 4.5996eV. The evaluated zero point of potential energy is located at the bond length of 2.1206Å. Compared with the experiment, the calculated vibrational constant ω_e and $\omega_e\chi_e$ are 12.1cm^{-1} and 0.05cm^{-1} smaller, while $\omega_e\chi_e$ is 0.04cm^{-1} larger than the available observed values [3].

The first excited state $a^3\Pi$ and $A^1\Pi$ arises from the electronic configuration $1\sigma^2 2\sigma^2 3\sigma^\alpha 4\sigma^0 5\sigma^0 1\pi^4 2\pi^\alpha$, which results from the $3\sigma \rightarrow 2\pi$ excitation from electronic configuration of the ground state. $a^3\Pi$ state has the dissociation energy of 1.0205eV and 23 vibrational levels are included. The energy minimum of 28878.9242 cm^{-1} at the equilibrium internuclear distance of 2.1750Å is a little lower than the experimental value of 29005.4cm^{-1}.

Under the influence of the spin-orbit interaction, the state $a^3\Pi$ could split to four Ω states (0^+, 0^-, 1 and 2), which will be discussed in detail in next section. It should be noted that the state $A^1\Pi$ has two very shallow potential wells, which is due to the avoided crossing between the state $A^1\Pi$ and $^1\Pi$(II). The one at the shorter bond length of 2.7730Å is 0.08835eV and the other at the longer bond length of 3.9215Å is 0.0467eV.

The excitation configuration of $1\sigma^2 2\sigma^2 3\sigma^2 4\sigma^0 5\sigma^0 1\pi^3 2\pi^1$ acts as main configuration of $^1\Sigma^-$, $^3\Sigma^-$, $^1\Sigma^+$(II), $^3\Sigma^+$(II), $^1\Delta$, $^3\Delta$ and $^3\Sigma^+$(I). Among these state, only $^3\Sigma^+$ (II) is a fully repulsive state. The remaining states all hold the potential wells with the depths around 1eV. The PECs of $^1\Sigma^-$ and $^1\Delta$ are nearly completely overlapped. Therefore, the corresponding spectroscopic constants are also nearly same. The excitation energies of T_e are 29948.7282cm^{-1} and 29825.4689cm^{-1} respectively. The difference between equilibrium internuclear distances is mere 0.0045Å and the calculated difference between the vibrational constant ω_e is mere 1.1cm^{-1}. Similarly, the spectroscopic constants of $^3\Delta$ state also conform to these of the state $^3\Sigma^-$.

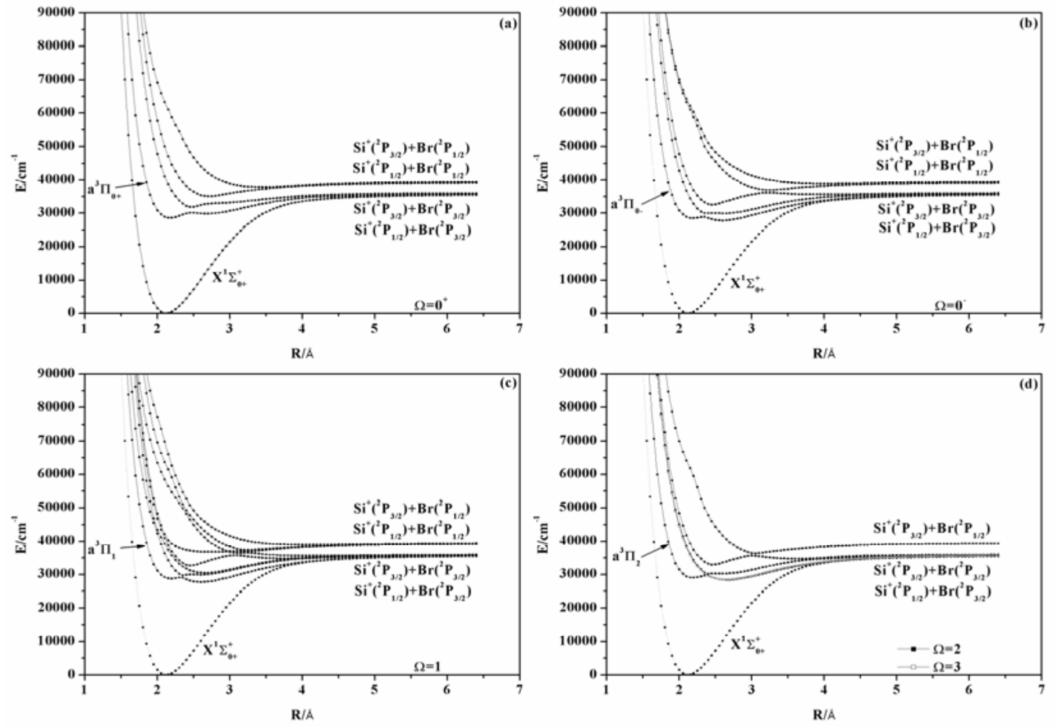

Fig. 2: The PECs for the 23 Ω states of $SiBr^+$ cation as functions of internuclear distance R.

The electron states $^3\Pi$(II) and $^1\Pi$(II), resulting from the main electronic configuration $1\sigma^2 2\sigma^2 3\sigma^2 4\sigma^\alpha 5\sigma^0 1\pi^{\alpha\beta\alpha} 2\pi^0$ and $1\sigma^2 2\sigma^2 3\sigma^\alpha 4\sigma^0 5\sigma^0 1\pi^4 2\pi^\alpha$, both hold a particular shallow potential well. The well depth of the state $^3\Pi$ (II) is only 0.0921eV and the well contains 8 vibrational levels. The evaluated dissociation energy D_e of $^1\Pi$ (II) is 0.033eV and the excitation energy of 36561.97cm^{-1} is somewhat larger than that of the $^3\Pi$ (II) state.

Table 2 The dissociation limits of Ω electronic states

Ω States	Si$^+$+Br	Energy/cm^{-1}	
		This work	Exp^a
2, 1, 1, 0^+,0^-	$^2P_{1/2}$+$^2P_{3/2}$	0	0
3, 2, 2, 1, 1, 1, 0^+,0^+,0^-,0^-	$^2P_{3/2}$+$^2P_{3/2}$	277.12	287.24
1, 0^+,0^-	$^2P_{1/2}$+$^2P_{1/2}$	3652.57	3685.24
2, 1, 1, 0^+,0^-	$^2P_{3/2}$+$^2P_{1/2}$	3929.69	3972.48

^{a}Experimental values from the Ref[13]

Table 3 The spectroscopic constants of Ω state

Ω State	T_e/cm^{-1}	R_e/Å	ω_e/cm^{-1}	$\omega_e\chi_e$/cm^{-1}	B_e/cm^{-1}	D_e/eV	Dominant Λ-S composition at R_e (%)
X0^+	0	2.1205	525.90	1.617	0.1809	4.4402	X$^1\Sigma^+$(99.89)
	0^a		533.3±1.8^a	1.5±0.7^a			
	0^b		535.8^b	1.6^b			
1(I)	27713.18	2.6020	210.16	3.826	0.1201	1.0157	$^3\Sigma^+$(I)(81.68), $^3\Sigma^-$(17.58)
Well(II)	**28741.67**	**2.1875**	**392.33**	**7.238**	**0.1712**	**0.8616**	**a$^3\Pi$(97.01), $^3\Sigma^+$(1.44)**
	29140±5^a		392±3.7^a				
0^-(I)	27828.49	2.6005	199.2185	4.137	0.1202	1.0245	$^3\Sigma^+$(I)(84.10), $^1\Sigma^-$(14.38), a$^3\Pi$(1.5)
Well(II)	**28473.46**	**2.1845**	**373.1320**	**15.5471**	**0.1720**		**a$^3\Pi$(96.62), $^3\Sigma^+$(I)(2.79)**
2(I)	28363.10	2.6620	217.41	6.255	0.1148	0.9549	$^3\Delta$(58.99), $^1\Delta$(40.92)
Well(II)	**29036.93**	**2.1880**	**386.0866**	**3.6752**	**0.1708**	**0.8714**	**a$^3\Pi$(99.94)**
3	28409.03	2.6455	219.8925	1.514	0.1162	0.9336	$^3\Delta$(100)
0^+(II)	28571.67	2.1775	415.7812	5.010	0.1716	0.9062	a$^3\Pi$(99.24)
	29005.4^b		428.7^b	6.9^b			
Well(II)	**29830.14**	**2.6740**	**194.5518**	**4.9367**	**0.1148**	**0.7502**	**$^3\Sigma^-$(91.21), $^1\Sigma^+$(II)(1.58)**
1(II)	29761.80	2.3560	110.83	5.341	5.4505	0.7841	a$^3\Pi$(61.47), $^3\Sigma^+$(I)(18.00), $^3\Sigma^-$(11.96), $^3\Delta$(8.1)
0^-(II)	29926.00	2.6215	112.8683	4.672	0.1172	0.7671	$^1\Sigma^-$(70.94), a$^3\Pi$(20.82), $^3\Sigma^+$(14.38)
2(II)	30187.19	2.4059	381.28	--------	0.1248	0.7314	a$^3\Pi$(64.08), $^1\Delta$(35.91)
1(III)	30477.25	2.6635	208.00	1.624	0.1147	0.6885	$^3\Sigma^-$(64.65), $^3\Sigma^+$(I)(14.13), $^3\Delta$(13.58), A$^1\Pi$(7.62)
0^+(III)	31827.86	2.4670	342.81	14.833	0.1340	0.5216	$^3\Sigma^-$(58.65), a$^3\Pi$(36.48),

							$^1\Sigma^+$(II)(4.69)
0^-(III)	32470.97	2.4550	405.3670	10.278	0.1350	0.4419	$^1\Sigma^-$(47.13), $^3\Sigma^+$(I)(13.3), $a^3\Pi$(39.56)
1(IV)	32673.05	2.4550	431.81	19.285	0.1351	0.4156	$a^3\Pi$(39.62), $^3\Sigma^-$(29.64), $^3\Delta$(22.22)
2(IV)	32985.77	2.4655	386.91	18.194	0.1339	0.3798	$^3\Pi$(II)(100)
0^+(IV)	35034.82	2.7115	259.29	6.200	0.1107	0.5354	$^1\Sigma^+$(II)(60.56), $a^3\Pi$(31.64), $^3\Sigma^-$(6.75)
1(V)	35634.23	4.0855	45.10	1.410	0.0487	0.0590	$^3\Sigma^+$(II)(47.11), $A^1\Pi$(30.53), $a^3\Pi$(20.37)
2(III)	36409.73	3.0490	242.45	7.476	0.0877	0.3991	$a^3\Pi$(71.24), $^3\Pi$(II)(17.94), $^3\Delta$(5.45), $^1\Delta$(5.38)
1(VI)	36892.58	3.2500	125.34	0.476	0.0759	0.3100	$^3\Pi$(II)(39.57), $A^1\Pi$(23.66), $a^3\Pi$(10.20), $^3\Delta$(8.2), $^1\Pi$(II)(3.78)
0^-(IV)	36895.25	3.2440	191.6572	5.651	0.0774	0.3097	$^3\Pi$(II)(69.18), $^3\Sigma^+$(II)(12.8), $a^3\Pi$(9.18),$^1\Sigma^-$(4.62), $^3\Sigma^+$(I)(4.22)
1(VII)	37394.3508	3.2260	156.46	4.014	0.0776	0.2799	$A^1\Pi$(47.42), $^1\Pi$(II)(30.24), $^3\Sigma^+$(II)(5.29), $^3\Sigma^-$(4.63), $^3\Pi$(II)(4.46), $^3\Sigma^+$(I)(3.98), $^3\Delta$(3.0)
0^+(V)	37803.24	3.4630	107.54	1.750	0.0679	0.2240	$a^3\Pi$(53.62), $^3\Pi$(II)(33.82), $^1\Sigma^+$(II)(9.50), $X^1\Sigma^+$(2.91)
0^-(V)	38885.19	4.0000	50.4959	1.1605	0.0508	0.1002	$^3\Sigma^+$(II)(52.98), $a^3\Pi$(46.52)
1(VIII)	38921.7267	4.0630	47.9329	1.125	0.0492	0.1020	$^3\Sigma^+$(II)(50.25), $A^1\Pi$(23.24),$a^3\Pi$(22.86), $^1\Pi$(II)(2.69)

[a]Ref[3] [b]Ref[5]

b. The PECs and spectroscopic constants of Ω states

Once the spin-orbit coupling effect is introduced into the calculation, 23 Ω states are generated from the 12 Λ-S states including 5 Ω states of 0^+ symmetry, 5 Ω states of 0^- symmetry, 8 Ω states of symmetry, 4 Ω states of 2 symmetry and 1 Ω states of 3 symmetry. **Fig. 2** displays the potential energy curves of computed Ω states, while **Table 2** shows the dissociation relationship of the calculated Ω states. These 23 Ω states are respectively correlated to the dissociation limits of $Si^+(^2P_{1/2})+Br(^2P_{3/2})$, $Si^+(^2P_{3/2})+Br(^2P_{3/2})$, $Si^+(^2P_{1/2})+Br(^2P_{1/2})$ and $Si^+(^2P_{3/2})+Br(^2P_{1/2})$, which are generated from the original dissociation limit of $Si^+(^2P_u)+Br(^2P_u)$. The calculated energy intervals of $Si^+(^2P_{1/2})$-$Si^+(^2P_{3/2})$ and $Br(^2P_{3/2})$-$Br(^2P_{1/2})$ are respectively 247.56cm^{-1} and 3652.50cm^{-1}, which are in accord with the corresponding experimental values[13] of 287.24cm^{-1} and 3685.24cm^{-1}. The spectroscopic constants of the bound Ω states are determined and listed in **Table 3**. The spectroscopic constants of bound Ω states and their dominant Λ-S state compositions at R_e are given in **Table 3**. With the increasing of bond lengths, the states which have the same Ω components will mix, and the compositions of these bound Ω states will become more complex.

The ground bound $X0^+$ state of $SiBr^+$ is mainly generated from the Λ-S state $X^1\Sigma^+$. And it is uninfluenced by SOC effect in the bound area. Therefore the spectroscopic constants can well reproduce with these of the state $X^1\Sigma^+$. The evaluated dissociation energy D_e of 4.4402eV becomes 0.16eV lowers than the original value after considering the SOC effect.

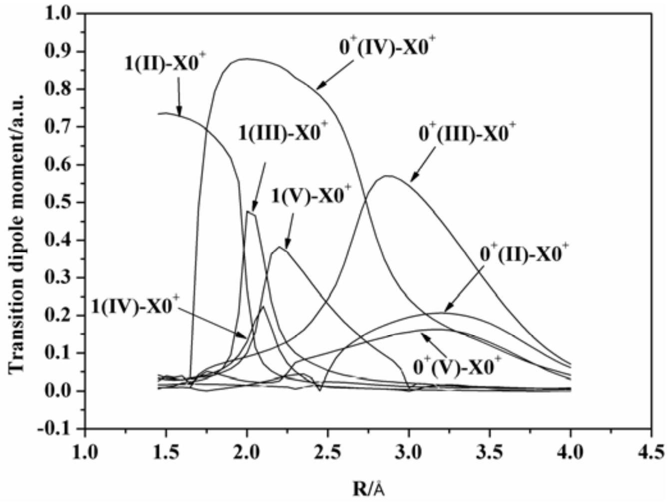

Fig.3: The TDMs from excited states of 1 and 0^+ symmetries to $X0^+$ state.

The first excited state $a^3\Pi$ splits into four Ω states including $a^3\Pi_{0-}$, $a^3\Pi_{0+}$, $a^3\Pi_1$ and $a^3\Pi_2$ by the spin-orbit interaction. At the equilibrium position of Λ-S state $a^3\Pi$, their energy arrangement from low to high is $a^3\Pi_{0-}$, $a^3\Pi_{0+}$, $a^3\Pi_1$ and $a^3\Pi_2$. The excitation energy intervals of $a^3\Pi_{0-}$-$a^3\Pi_{0+}$, $a^3\Pi_{0+}$-$a^3\Pi_1$ and $a^3\Pi_1$-$a^3\Pi_2$ are 98.21cm^{-1}, 170cm^{-1} and 295.26cm^{-1} respectively. The crossing region of $a^3\Pi$ yields many avoided crossings with the SOC added. As shown in **Fig. 2**, the potential energy curves of the state 1(I), 0^-(I), 2(II) and 0^+(II) have two potential wells. The corresponding spectroscopic constants of the two well are also listed in **Table 3**. For the state 1(I), as shown in **Table 3**, The wells at shorter R_e are all mainly consist of the Λ-S state $a^3\Pi$, while the wells at longer R_e are mainly from the Λ-S state $^3\Sigma^-$. The energy minima of the potential well(I) is 1028cm^{-1} lower than that of the well(II) and the R_e of the former is much smaller than that of the latter. However, the spectroscopic constants fitting of the well (II) is coincident with the experimental data. As far as we know, no new spectroscopic data for 1(I) state in the experiment have been reported to date. Therefore, it is recommended that more accurate experimental measurements on those Ω states should be performed.

In the SOC calculation, only one Ω=3 state is calculated, which is purely generated from the electronic state $^3\Delta$ over the internuclear distances. Therefore, the corresponding PEC is smooth and similar to that of the Λ-S state $^3\Delta$. Compared with the spectroscopic constants of $^3\Delta$ state, T_e value of Ω=3 state is 228.93 cm^{-1} lower, and the vibrational constant ω_e is 17.9 cm^{-1} lower by the SOC effect. Meanwhile, the depth of the potential well becomes shallower by 0.1074eV.

After taking into account the SOC effect, it could be noted that most of PECs for Ω states are not smooth anymore and strongly different from original PECs of Λ-S states. The Ω states such as $a^3\Pi_{0-}$, $a^3\Pi_{0+}$, $a^3\Pi_1$ and $a^3\Pi_2$ generated from $a^3\Pi$ state hold an unsmooth point located at the bond length about 2Å, which could be owing to the avoided crossing between $a^3\Pi$ and $^3\Pi$(II).

c. The TDMs for several transitions of 0^+-X0^+ and 1-X0^+ types

Fig. 3 shows the transition dipole moments (TDMs) as the functions of the internuclear distance between the Si^+ and Br atoms, in which these transitions can be divided into two types, namely, 0^+-X0^+ and 1-X0^+ allowed transition. The 0^+(IV)-X0^+ transition owns the largest TDM peak value of 0.88a.u. at R=2.0Å, where the 0^+(IV) state at the peak comes from the Λ-S state $^1\Sigma^+$(II) and the $^1\Sigma^+$(II)-$X^1\Sigma^+$ belongs to the singlet-singlet allowed transition. Similiarly, the 0^+(III)-X0^+, 0^+(II)-X0^+ and 0^+(V)-X0^+ also have their own peaks and the TDM values are located at the bond length of 2.8Å, 3.2Å and 3.23Å, respectively. The remaining transitions of 1-X0^+ type, 1(II, III, IV, V)-X0^+, also hold the larger TDM values, where the TDM of 1(II)-X0^+ is reduced strongly with increase of bond length from 1.5 to 2.5Å.

Conclusion

The calculations of entirely 12 Λ-S states of $SiBr^+$ are carried out with the internally contracted multi-reference configuration interaction (MRCI) plus Davidson modification(+Q) at the theoretical level of uncontracted all-electron aug-cc-pVTZ basis set, where the Douglas- Kroll scalar relativistic effect is taken into account. The spin-orbit coupling effect is introduced to make the 12 Λ-S states split and recombine to 23 Ω states. These Λ-S states and the corresponding spectroscopic constants are firstly reported except the ground state $X^1\Sigma^+$ with the lowest two excited states $a^3\Pi$ and $A^1\Pi$. Here our theoretical results for the electronic states $X^1\Sigma^+$, $a^3\Pi$ and $A^1\Pi$ are in good agreement with the observed values. The transition dipole moments (TDMs) of the transitions from the excited Ω states of 0^+ and 1 symmetries to the ground Ω state are predicted for the first time, where the TDM for the electron state 0^+(IV) to the ground state X0^+ located at the bond length about 2.0Å is larger than those of the remaining transitions.

Acknowledgments

This work is supported by the National Natural Science Foundation of China (Grant No. 112 74096), Innovation Scientists and Technician Troop Construction Projects of Henan Province (Grant No. 124200510013) and the Base and Cutting-edge Technology Research Projects of H enan Province (Grant No. 132300410428).

Reference

[1] J. W. Coboum, H. F. Winters, Plasma etching—A discussion of mechanisms, J. Vacuum, Sci. Technol., 16(1979), 391.

[2] X. M. Zhang, H.S. Zhai,Y. F. Liu, J. F. Sun, Extensive *ab initio* calculation on low-lying excited states of CCl^+ including spin-orbit interaction, J. Quant. Spectros. RA., 119(2013), 23-31.

[3] M. Tsuji, K. Shinohara, S. Nishitani, T.Mizuguchi, Y. Nishimura, Emission spectra of group IV monohalide ions: $^3\Pi^1$-X $^1\Sigma^+$ emissions of $SiBr^+$, Can. J. Phys., 62(1984), 353-360

[4] M. Ishiguro, T. Okabayashi, M. Tanimoto, Microwave spectroscopic study of the BBr molecule, J. Mol. Struct., 352 (1995), 317-323

[5] K. P. Huber, G. Herzberg, Molecular Spectra and Molecular Structure IV: Constants of Diatomic Molecules, Van Nostrand Reinhold, New York, 1979

[6] H. J. Werner, P. J. Knowles, *et al.*, MOLPRO, a package of *ab initio* programs, Version 2008.1, http://www.molpro.net.

[7] R. J. Le Roy, LEVEL 8.0: A Computer Program for Solving the Radial Schrödinger Equation for Bound and Quasibound Levels, University of Waterloo Chemical Physics Research Report CP-663 (2007).

[8] H. J. Werner, P.J. Knowles, A second order multi-configuration SCF procedure with optimum convergence, J. Chem. Phys., 82 (1985), 5053-5063.

[9] P. J. Knowles, H. J. Werner, An efficient second-order MCSCF method for long configuration expansions, Chem. Phys. Lett., 115 (1985), 259-267.

[10] H. J. Werner, P.J. Knowles, An efficient internally contracted multiconfiguration-reference configuration interaction method, J. Chem. Phys., 89 (1988), 5803-5814.

[11] P.J. Knowles, H. J. Werner, An efficient method for the evaluation of coupling coefficients in configuration interaction calculations, Chem. Phys. Lett., 145 (1988), 514-522.

[12] A. Berning, M. Schweize, H. J. Werner, Spin-orbit matrix elements for internally contracted multireference configuration interaction wavefunctions, Mol. Phys., 98 (2000), 1823-33.

[13] C. E. Moore, Atomic Energy Levels, National Bureau of Standards, Washington, DC, 1971.